FLUTTER OPTIMIZATION OF LARGE TRANSPORT AIRCRAFT

Gregory D. Sikes*, George T.J. Tzong**, Anil K. Sharma#
Douglas Aircraft Company, McDonnell Douglas Corporation
Long Beach, California

Abstract

Flutter is a critical behavior parameter involving a large number of design variables that must be considered very early in the design cycle. The complexity of modern aircraft structures and their models makes automation of the flutter design procedure essential. This paper presents flutter optimization of three different aircraft models using the Aeroelastic Design Optimization Program (ADOP) developed at the Douglas Aircraft Company. These studies focus on the design of structural parameters, such as beam bending stiffness, skin thickness, stringer area, lumped mass value and offset, engine location and pylon stiffness to satisfy the flutter requirements while minimizing weight. Some basic finite element technology, related to optimization, are summarized. Flutter optimization topics including case control logic, flutter analysis, design sensitivities, modal analysis, and design of general stiffness/flexibility elements are also discussed.

Introduction

Aircraft structural design and related product development is a complicated process which requires interaction among various design disciplines including static strength, flutter, dynamics, aeroservoelasticity, loads, allowables, etc. Current practice is to size the aircraft for these conditions in "series". Frequently, the quality and accuracy of the results from the diverse disciplines are compromised because of the inconsistent modelling practices and insufficient communication between the discipline groups. Furthermore, as many design iterations are required, a tremendous amount of labor and time is involved. In order to improve this process and reduce the design cycle time, different analysis and design disciplines and associated computer programs should be integrated so that the aircraft structural design can be completed using a unified, multidisciplinary design system.

Considering the recent advances in computational methods and computer hardware and recognizing the shortcomings in the present design process, the development of an aeroelastic design optimization program, ADOP[1] , has been undertaken at the Douglas Aircraft Company of the McDonnell Douglas Corporation. ADOP is being developed for efficient static, dynamic, and aeroelastic optimization of large, finite element, aircraft structural models. The program optimizes the models to achieve a minimum weight while simultaneously satisfying all structural performance requirements.

Presently, ADOP optimizes aircraft structural models subject to stress, displacement, modal frequency and flutter constraints. Static strength optimization ensures that the stresses are below the allowable values and the structural stiffness meets the deformation requirements subject to the design loads. Fully stressed design resizes each finite element using the ratio between actual and allowable stresses. The resultant model is then used in the more rigorous numerical optimization. Frequency constraints prevent the structural vibration modes from falling into a specific range of frequencies. Flutter constraints must be satisfied early in the design phase and have to consider all critical flight and payload conditions. In ADOP, flutter velocity of an aircraft is restrained to be above the design speed for all design conditions. (The design speed for subsonic, transport aircraft is $1.2V_d$ where V_d is the design dive speed.)

This paper focuses on the flutter optimization capabilities within ADOP. The first two sections summarize the finite element technology and flutter optimization details related to the case studies. Three different finite element models of large transport aircraft were studied, of which two were modelled with beam elements and the third by a full, 3-D, finite element wing with a corresponding beam model of the fuselage and tail.

The first example is a beam model with only four wing tip masses as the design variables. Three flight conditions, at different Mach numbers, were included in the flutter constraints.

Next, the 3-D finite element wing model with a beam fuselage and tail is simultaneously optimized for stress and flutter. Stress optimization will just be mentioned and the focus of this study will be on two different optimization runs, one stress critical and the other flutter critical, and the different resulting designs.

---

* Senior Engineer/Scientist
** Principal Engineer/Scientist, Member AIAA
# Engineer/Scientist Specialist

The third example, a beam model, was intensively studied for flutter optimization. Different design variables including wing stiffness, engine location, pylon stiffness and wing tip mass are individually investigated for their ability to satisfy the flutter criteria while minimizing weight. A combination of all the design variables are then tested to observe the interaction that occurs while trying to satisfy the flutter constraint.

Finite Element Technology

The following discusses the finite element technology available in ADOP with respect to optimization. Elements, their design variables and design variable linking are presented.

Finite Elements

The finite elements in ADOP's library that can be designed include 2-node rod and bar, linear and torsional springs, 3-node triangular membrane and plate-shell elements, 4-node hybrid quadrilateral membrane and plate-shell elements, quadrilateral shear panel, 3 and 4-node composite membrane elements, lumped mass element, and general flexibility/stiffness element. (Also available for analysis are 3 and 4-node composite shell elements and an 8-node solid.) Rigid elements and multiple point constraint capabilities are also implemented to provide modelling flexibility.

Design variables for bending beams can be the real dimensions of the cross section, for example the flange thickness and height of a J-shaped beam, or the more general cross section area and moments of inertia. Spring elements are provided for modelling convenience of special aircraft components (flap hinges, etc.); spring stiffness coefficients can be designed. The mass element is used to simulate the weight of non-structural components such as landing gears, engines, etc. Its design variables are the scalar mass and offset from a node. The 3 and 4-node membrane and shell elements have constant thickness and homogenous orthotropic material properties. Their design variable is thickness. Composite membrane elements, 3 and 4-node, can have each ply independently oriented from the others. Membrane type elements are used for panels which are dominated by inplane stresses. The composite membrane design variables are the individual, lumped sum, ply thicknesses and the global orientation angle of a composite panel.

Design Variable Linking

When a finite element model is used in the design process, the structural performance is influenced by every finite element; their effects must be known when a particular constraint is to be satisfied. In the optimization process the number of design variables is limited by computer resources. It is impractical and unnecessary to retain each element as an independent design variable, since in portions of a structure a simple relationship of structural properties can be defined. For example, a long rod with linearly varying cross section area can be defined by the values at both ends; elements anywhere in the rod have cross section areas defined as a linear combination of the two end areas. Similarly, in a panel region with a linearly varied thickness along the sides the four corner thicknesses can be used as independent design variables, and they in turn define the thickness of any panel element. This relationship, design variable linking[2], is primarily based on manufacturing constraints and users' design experience. The finite elements that can be represented by a few design variables and a shape function are grouped together and their sizes are expressed as

$$\underset{\sim}{t} = \underline{R}\,\underset{\sim}{D} \qquad (1)$$

where $\underset{\sim}{t}$ is the element size vector, $\underline{R}$ is the ratio between $\underset{\sim}{t}$ and the independent design variables $\underset{\sim}{D}$.

ADOP contains a comprehensive design variable linking scheme. Dependent finite element sizes are related to their independent design variable(s) through "scaling ratios". Ten different beam cross sections such as T, Z, I, etc., spring stiffness, membrane and bending plates, offset lumped mass, and a general element are designable in ADOP. In addition, free and fixed design variables for the same group are allowed so that, for example, panels can maintain a minimum thickness while any additional thickness will be adjusted for best design. Constant, linear, and bilinear shape functions are available to define element size variation. Additionally, user input variations are allowed which provide the capability for quadratic and higher order variation of element sizes within a design group. A graphics program is available to interactively define design groups while viewing the finite element model.

Flutter Optimization Technology

The complexity of modern aircraft structures and their models makes automation of the flutter design cycle essential. An aircraft has to be designed flutter-free for all payloads and altitudes. This section presents the technology employed in ADOP with respect to flutter optimization.

Analysis and Design Sensitivities

An accurate and efficient modal analysis is essential to various dynamic evaluations of structures. Today, large finite element models are commonly used to simulate the dynamic behavior of structures. ADOP offers a unique block Lanczos method[3,4,5] and accelerated subspace iteration[6,7] for modal analysis. Both methods are designed to directly extract eigenvalues and eigenvectors of large models and are implemented with numerical error correction techniques to retain accuracy and avoid repeated roots.

Flutter analysis is performed with the modal approach. Structural characteristics are simulated by a number of vibration modes and the number of modes should be sufficient to represent the true behavior of the aeroelastic system. Both the k (V-g) and p-k flutter analysis methods are available in ADOP. However, only the k-method formulation will be discussed as all of the examples presented in this paper use this method. The k-method flutter equation is written as

$$[\underline{K} - \lambda_m(\underline{M} + \bar{\underline{A}})]\underline{U}_m = \underline{0} \tag{2}$$

where $\underline{K}$ and $\underline{M}$ are the generalized, or modal, stiffness and mass matrices, respectively. Hysteretic damping is included in $\underline{K}$ using a modal damping ratio. $\bar{\underline{A}}$ is the generalized aerodynamic influence coefficient matrix, which is obtained by pre- and post-multiplying the discrete aerodynamic matrix by the splined mode shapes from the structural nodal points to the aerodynamic grid points. (The discrete aerodynamic matrix is computed using the Doublet-Lattice method.[8,9]). λ_m and $\underline{U}_m$ are the complex eigenvalue and eigenvector of the aeroelastic system, respectively, and $\lambda_m = \omega_m^2/(1 + ig_m)$, where g_m is the damping of the system and ω_m is the circular frequency.

The above equation is solved step-by-step along the reduced velocity axis, 1/k. A flutter point, defined by modes with zero damping ratios, is obtained from a direct numerical search using the approximate locations of flutter points. The ADOP flutter analysis module directly computes the flutter velocity and frequency using the Laguerre method[10,11]. If more than one root is present, deflation is applied to avoid repeated detection of the same root. After the reduced frequency k is determined, the flutter velocity is obtained as

$$V = \frac{\omega_m b}{k} \tag{3}$$

where b is the half reference chord length.

In the ADOP flutter optimization a constraint is applied by imposing an allowable flutter speed. If the constraint is not satisfied, the structural finite elements have to be resized to increase the flutter speed to meet the design requirement. The flutter design sensitivity can be expressed as

$$\frac{\partial V}{\partial D_i} = \frac{b}{k}\frac{\partial \omega_m}{\partial D_i} - \frac{\omega_m b}{k^2}\frac{\partial k}{\partial D_i} \tag{4}$$

where $\partial\omega_m/\partial D_i$ and $\partial k/\partial D_i$ are the design sensitivities of frequency and reduced frequency at flutter, respectively. In the k-method, the two design sensitivities are computed by

$$\frac{\partial k}{\partial D_i} = -\frac{Im\left(\frac{1}{\omega_m^2}\underline{V}_m{}^T\frac{\partial \underline{K}}{\partial D_i}\underline{U}_m - \underline{V}_m^T\frac{\partial \underline{M}}{\partial D_i}\underline{U}_m\right)}{Im\left(\underline{V}_m^T\bar{\underline{A}}(k)\underline{U}_m\right)} \tag{5}$$

and

$$\frac{\partial \omega_m}{\partial D_i} = -\frac{\omega_m^3}{2}\left[\frac{\partial k}{\partial D_i}Re\left(\underline{V}_m^T\bar{\underline{A}}(k)\underline{U}_m\right) + Re\left(\underline{V}_m^T\frac{\partial \underline{M}}{\partial D_i}\underline{U}_m - \frac{1}{\omega_m^2}\underline{V}_m^T\frac{\partial \underline{K}}{\partial D_i}\underline{U}_m\right)\right] \tag{6}$$

where $Re(.)$ and $Im(.)$ are the real and imaginary parts of the enclosed quantity. $\underline{V}_m^T$ is the left eigenvector of Eq. 2. $\partial\underline{K}/\partial D_i$ and $\partial\underline{M}/\partial D_i$ are the design sensitivities of the generalized stiffness and mass matrices, respectively.

Design of General Elements

Structural components are sometimes modelled using flexibility and stiffness matrices, or GENEL's in NASTRAN[12] terminology. It may be desired to design the stiffness properties of a GENEL. For example, an engine pylon, modelled as a GENEL, will affect the flutter speed if its stiffness is altered.

An eigenvalue problem can be written to solve for the GENEL vibration frequencies.

$$\underline{K}\,\underline{\phi} = \underline{M}\,\underline{\phi}\,\underline{\Lambda} \tag{7}$$

where $\underline{K}$ and $\underline{M}$ are the stiffness and mass matrices, respectively, $\underline{\phi}$ is the matrix of eigenvectors and $\underline{\Lambda}$ is the vector of eigenvalues.

Because of the characteristics of GENEL's, the associated mass effects for the design procedure are not available. Instead, an identity matrix ($\underline{I}$) is used to replace the mass matrix in Eq. 7 by assuming that mass does not change during stiffness design. However, the weight penalty due to stiffness change is included in the design objective function but not in the modal and flutter analyses.

Premultiplying Eq. 7 by $\underline{\phi}^T$ and using $\underline{M} = \underline{I}$ yields

$$\underline{\phi}^T\underline{K}\,\underline{\phi} = \underline{\Lambda} \tag{8}$$

or,

$$\underline{K} = \underline{\phi}\,\underline{\Lambda}\,\underline{\phi}^T \tag{9}$$

The GENEL design variables are defined as the eigenvalues by assuming no change in the eigenvectors. Therefore, the sensitivities are written

$$\frac{d\underline{K}}{d\lambda_i} = \underline{\phi}_i\underline{\phi}_i^T \tag{10}$$

for i = 1,2,..,6.

When GENEL eigenvalues are designed for "each" DOF, the corresponding eigenvectors may not actually represent pure motion but rather a coupled motion between two or more DOF's. For example, an eigenvalue and corresponding eigenvector may actually represent a coupled forward/aft and vertical

translational motion whereas another set may represent pure lateral motion.

Optimization Strategy

Case control logic is used to guide the analysis and design flow and access appropriate discipline modules. The different disciplines currently available for design are flutter, stress, displacement and modal frequencies. ADOP allows for different boundary conditions of the same structure (symmetric and antisymmetric) along with multiple load cases, payloads and flight conditions (Mach and altitude). Case control is used to establish which analysis disciplines, and their related loads, payloads, boundary and flight conditions, are required during an optimization iteration. As the phrase "multidisciplinary" suggests, more than one discipline can be included in the design process.

The strategy is that the static strength, modal frequency and flutter analyses are performed between major iterations with the updated structure. Active and violated constraints from the analyses along with their design sensitivities are then collected for optimization. Including all active and violated constraints in the optimization procedure can be prohibitively expensive[13] ;therefore, in each design iteration only a subset of these constraints is selected. The constraints are evenly distributed among all design variable groups. Results from all boundary, payload and flight conditions and load cases are examined and inactive (very feasible) conditions are neglected in the next iteration to reduce computation. The method of modified feasible directions[13] in the optimization code DOT[14] is used in ADOP.

Numerical Studies

Three different aircraft, finite element models are used in the case studies on flutter optimization. The first case involves the design of mass elements to satisfy a flutter constraint for a beam model. Next, flutter optimization of a large, 3-D finite element model with bilinear design variable linking is presented. Finally, the last example studies flutter optimization by designing both individually and in combination beam bending stiffness, engine pylon stiffness, engine location and wing tip mass.

Case #1

This example uses a beam model of a transport aircraft. The flutter speed will be increased by adding non-structural mass outboard on the wing, forward of the leading edge spar. Four wing tip mass locations -- numbered one through four, inboard to outboard -- are modelled as lumped mass elements, each with an initial, insignificant mass of 0.0001 mugs. The optimizer is allowed to add mass at any of the four lumped mass positions, up to 1.0 mug (386.4 lbs.). A symmetric boundary condition is imposed. The first 18 dynamic modes were used in the flutter analysis including a 2.5% modal damping ratio.

To demonstrate flutter optimization with multiple flight conditions, the flutter constraint has to be satisfied for all three Mach numbers -- 0.8, 0.87, 0.90. The initial flutter speeds at these three conditions were below the design speed.

Figure 1 documents the design mass and flutter speed versus iteration. The optimization process required seven iterations for the three flight conditions to exceed the design flutter speed. Beyond that, the remaining iterations were spent attempting to reduce the weight of the model (the objective function). The final design value of the masses, from inboard to outboard, are 0.1120, 0.9555, 1.0, 1.0, respectively. As expected, from flutter engineers' experience, mass was added at the most outboard stations.

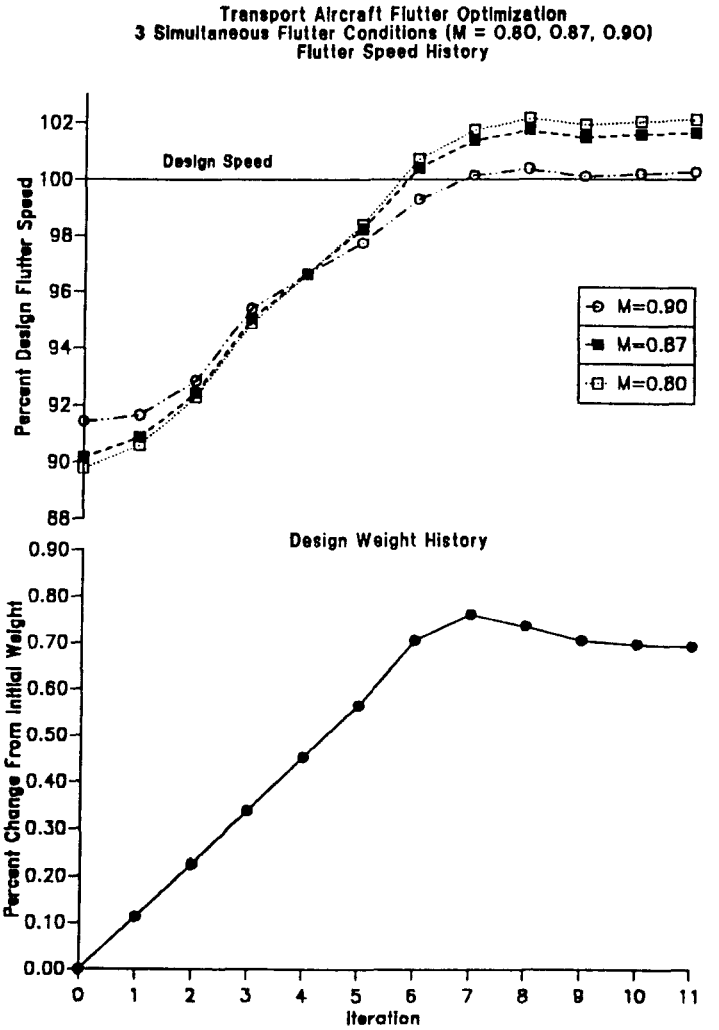

Fig. 1 - Flutter Optimization History -- 3 Flutter Cases

Case #2

This example demonstrates multidisciplinary optimization of a large, 3-D finite element model including bilinear design variable linking. Figure 2 shows a large transport model with a beam representation of the fuselage and tail and the wing as a full, finite ele-

ment model. The model is comprised of 9636 finite elements with 9580 degrees of freedom (DOF's).

The upper and lower wing panels and stringers contained within the wing box were designed to satisfy both stress and flutter constraints. (We will just mention here the stress constraint aspect and focus on the flutter.) As nearly 1000 skin and stringer elements exist in the design group, design variable linking became necessary to reduce the size of the problem. Experienced stress engineers report that the center wing area will have the thickest skin. To accommodate this

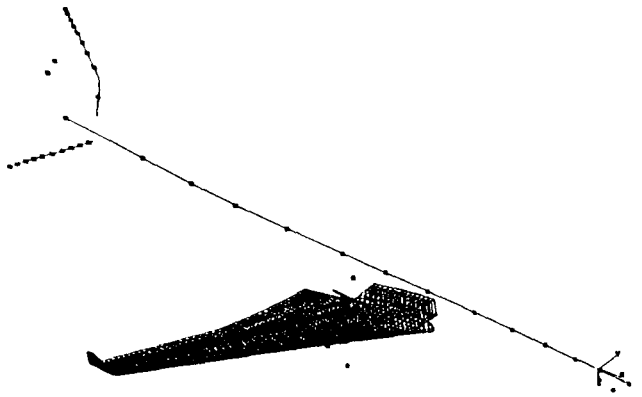

Fig. 2 - Transport Aircraft With 3-D Finite Element Wing

design trend, the wing box was divided into two chordwise design groups for the skins and stringers separately on the lower and upper surfaces. Additionally, the wing box was divided into five spanwise design groups with the boundaries corresponding to span breaks (Fig. 3). The four corner elements of

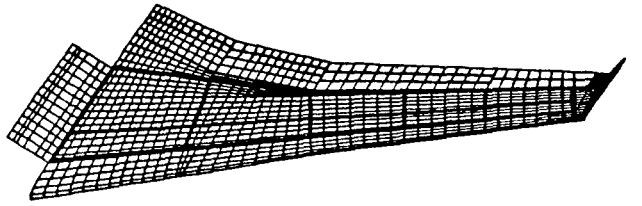

Fig. 3 - Bilinear Design Variable Linking Groups

each group are specified to be the independent design variables; a linear variation of thickness and area are defined between each corner variable. Separating the wing box into two chordwise groups with linear variations along the edges allows for the skin and stringer designs to have proper values at the leading and trailing edges and in the center box. With 10 bilinear design groups on the lower and upper wing defined for both skins and stringers, there are 160 design variables.

Two optimizations were performed on this model, both using the same stress criteria but with different flutter design speeds. The initial design run had a lower constrained flutter speed than the second. The stress criteria included material, buckling, and two-bay crack allowables. Buckling and two-bay crack allowables, a function of skin thickness and stringer area, were updated after each design iteration.

The first optimization run (Run #1), with the lower flutter speed constraint, was initiated with two fully stressed design (FSD) iterations and followed by numerical optimization. Two numerical optimization iterations were required to increase the flutter speed above the design speed (Fig. 4). Three additional iterations were spent addressing the stress constraints. This run was stress critical as the final design was well above the design flutter speed. To produce a flutter critical design and to compare the difference between a flutter critical and stress critical design, the second run (Run #2) was performed by raising the design speed (Fig. 4). After two FSD iterations, four numerical optimization iterations were required before the design speed was exceeded. The remaining iterations (7 - 13), prior to convergence, were used to reduce weight.

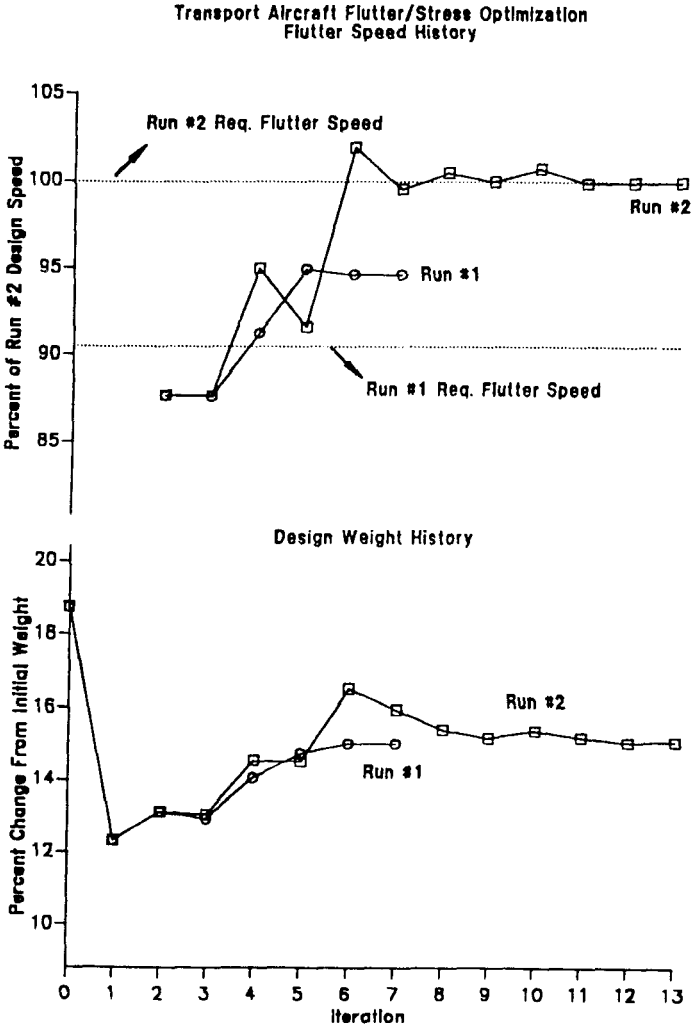

Fig. 4 - Flutter Optimization History -- 3-D Wing Model

This second optimization run resulted in a flutter critical design as the speed versus iteration shows that

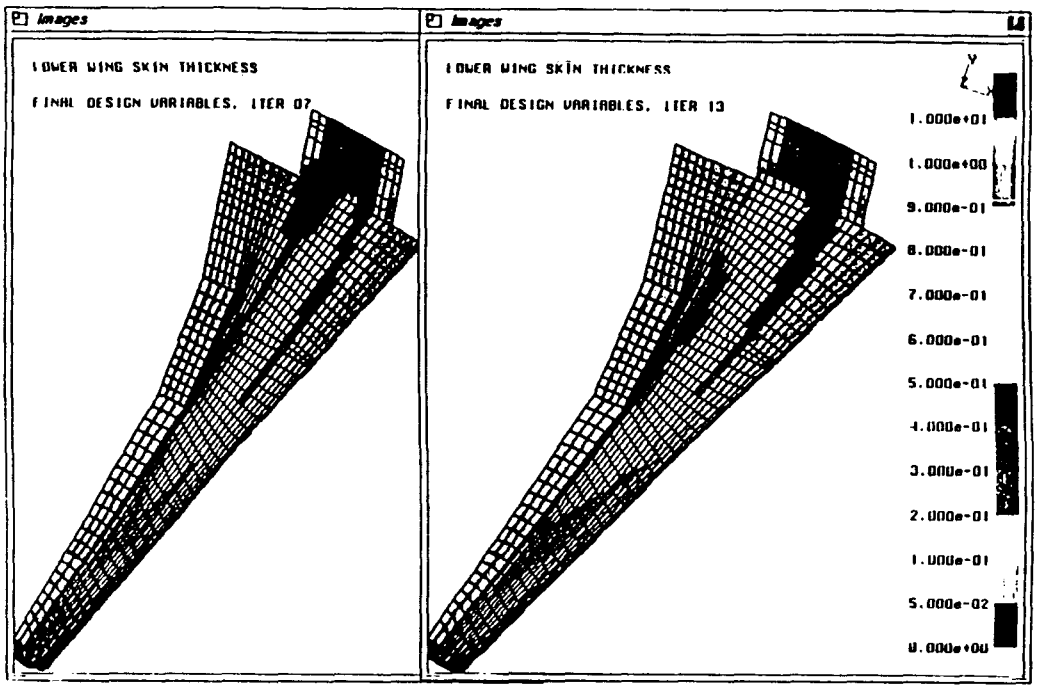

Fig. 5 - Stress vs. Flutter Critical Skin Thickness

the actual speed remains at the design speed constraint.

From Fig. 4, it appears that the weight for Run #1 converges toward the final design weight for Run #2; or, the final weight for the flutter critical design was approximately that of the stress critical design for the conditions imposed. A trade-off in design between the two conditions was observed in Figs. 5 and 6. Comparing the final skin and stringer designs for the stress and flutter critical designs for the lower wing surface, we see that, for the flutter critical design, the skin thickness was dramatically increased at the trailing edge root and slightly in the center wing area. Additionally, we note that the stringer areas were reduced at the trailing edge root and slightly in the center wing area. Thus, we see that skin thickness was increased in some areas for added torsional stiffness to increase the flutter speed. To offset the additional weight and stiffness due to increased skin thickness, the stringer areas were reduced in these areas.

Case #3

This third example is composed of several case studies in flutter optimization. The model is a symmetric, half-model, beam representation of a transport aircraft. Beam mass is discretized as mass elements at reference points. Two wing engines are modelled as mass elements and their pylons modelled with GENEL's. Only the wing and its components were considered in the design process. Different studies were performed to affect the flutter speed which included wing bending/torsional stiffness, pylon stiffness, engine location and wing tip mass. Among them, two optimization runs were performed by combining these design variables.

Wing Stiffness

One flutter optimization study was to design the wing beam vertical bending stiffness (I_y). Torsional stiffness, J, was linearly proportional to I_y. (The fore/aft stiffness was fixed.) Instead of using an actual stiffness value in design, the percentage change in stiffness was used as a design variable as we found that the design moved much more quickly towards feasibility. The original stiffness was defined as a fixed design variable.

For an increase in stiffness, a corresponding weight penalty exists. A weight penalty function was calculated based on I_y. Each beam's area (which contributes to mass) was related to the vertical bending stiffness by computing a ratio, C_s, of beam weight per unit length divided by the initial bending stiffness, or

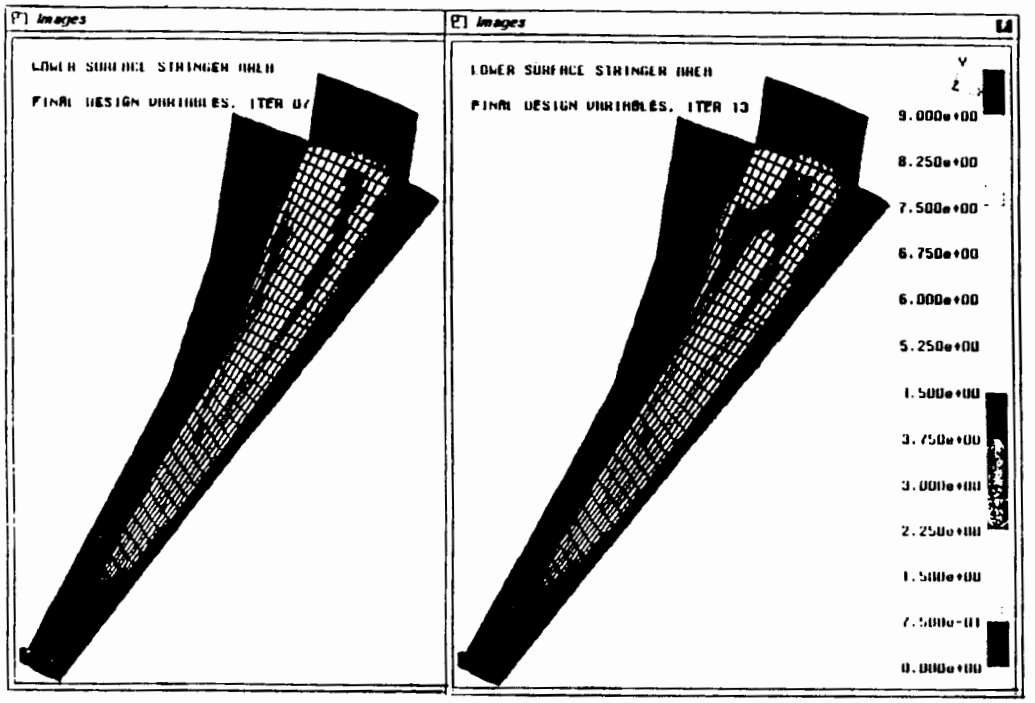

Fig. 6 - Stress vs. Flutter Critical Stringer Area

$$C_a = (m/l) / I_{yo} \qquad (11)$$

where (m/l) is the beam mass per unit length and I_{yo} is the initial vertical bending stiffness.

Using the percent change in I_y , the design variable relationship is written as

$$\begin{bmatrix} A \\ I_y \\ I_z \\ J \end{bmatrix} = \begin{bmatrix} C_a' \\ I_{yo} \\ 0.0 \\ J_o \end{bmatrix} [I_y'] + \begin{bmatrix} A_o \\ I_{yo} \\ I_{zo} \\ J_o \end{bmatrix} \qquad (12)$$

where $C_a' = C_a \times I_y$ and I_y' represents the percent change in the wing vertical bending stiffness.

The weight and flutter speed versus iteration results are shown in Fig. 7. Fig. 8 shows the final percent change in I_y along the wing span. Additionally, the beams between the inboard and outboard engines have the most impact on flutter speed per design change.

Wing Engine Pylon Stiffness

Adjusting the wing engine pylon stiffness will affect the flutter speed. The pylons are modelled as flexibility matrices, or GENEL's, and connect the engine masses to the wing structure. Pylon and engine masses are modelled by lumped mass elements. A technique for designing GENEL's stiffness was discussed in the section Flutter Optimization Technology.

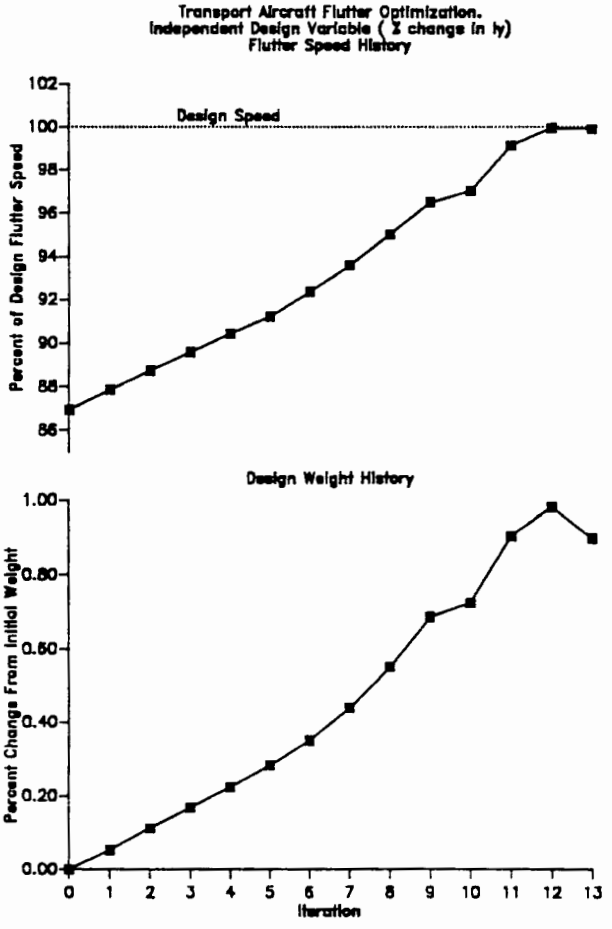

Fig. 7 - Flutter Optimization History -- Wing Stiffness

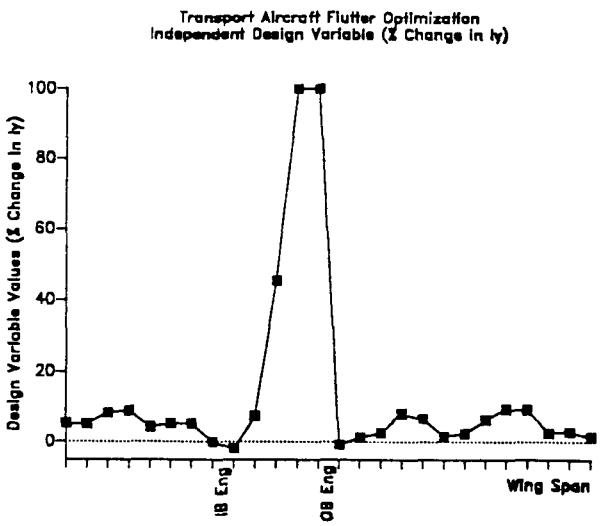

Fig. 8 - Optimized Wing Vertical Bending Stiffness Distribution

The design variables are the percentage value of the original eigenvalues (or stiffnesses) in each of the six DOF's (three translational and three rotational). For example, a design value of 1.25 translates into a 25% increase in pylon stiffness in the associated direction. The pylon stiffnesses were allowed to decrease 20% and increase 50%. (In the combination case presented later, pylon stiffness is not allowed to decrease.)

As mentioned earlier, it is difficult to include mass effects when designing pylons. Therefore, the penalty weight due to pylon stiffness change is included in the design objective function but not in the modal and flutter analyses. The penalty function is determined from the original pylon bending material mass. As the pylon eigenvalues are increased, so are the stiffnesses and thus the mass. For translational DOF's, the mass penalty is the percentage increase in stiffness times the original bending material mass; or, a 100% increase in stiffness for a particular direction results in a doubling of the associated material mass.

To include a weight penalty for added rotational stiffness, we assumed the rotational DOF's would have a lesser weight penalty and assigned 1/10 the translational penalty value to each DOF. In equation form, the mass penalty function is written

$$\Delta M = \begin{bmatrix} M_p & M_p & M_p & \frac{M_p}{10} & \frac{M_p}{10} & \frac{M_p}{10} \end{bmatrix} \begin{bmatrix} \lambda_x' \\ \lambda_y' \\ \lambda_z' \\ \lambda_{xx}' \\ \lambda_{yy}' \\ \lambda_{zz}' \end{bmatrix} \quad (13)$$

where M_p is the bending material mass associated with a particular direction and λ_i' is the percentage of the original eigenvalue associated with the i^{th} dof (x,y,z, $\theta_x,\theta_y,\theta_z$).

Fig. 9 shows the weight and flutter speed versus iteration for the pylon design. The outboard pylon lateral stiffness and all three rotational stiffnesses were increased to their upper limits while all other stiffnesses, including the inboard pylon, were decreased to the lower limits. We note that the flutter design speed is not satisfied and conclude that pylon stiffness, by itself, would not completely address the flutter concern.

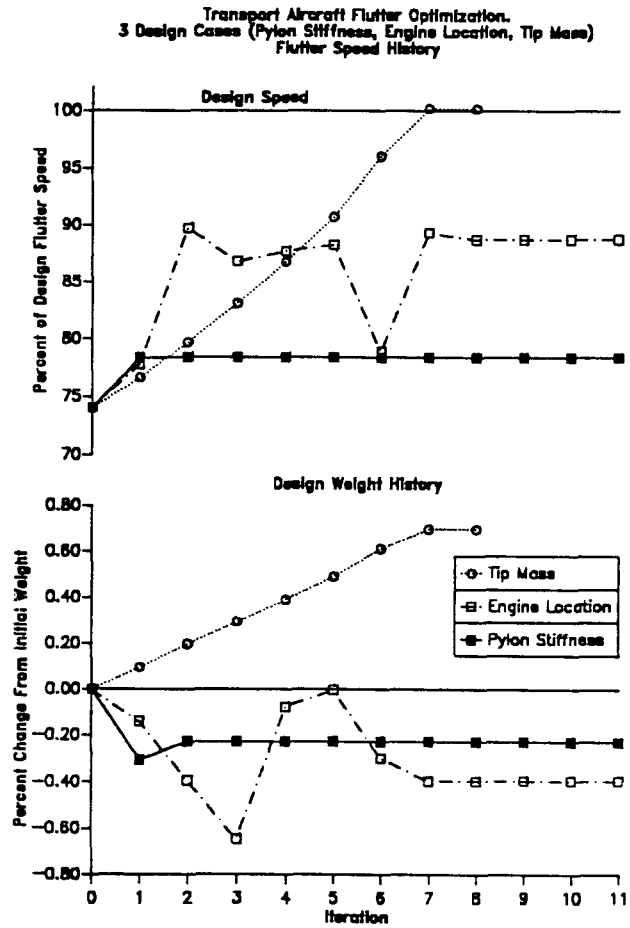

Fig. 9 - Flutter Optimization History -- Pylon Stiffness, Engine Location, and Wing Tip Mass Cases

Wing Engine Location

Adjusting the locations of the wing engines certainly will affect the flutter speed of an aircraft. In this particular study, only the fore/aft and vertical engine locations were designed. The engines were modelled with mass elements -- a mass value with an offset -- the design variables were the fore/aft and vertical offset from the original offset position.

A mass penalty function was defined as

$$\Delta M_e = - M_{ey}\Delta y - M_{ez}\Delta z \quad (14)$$

where M_{ey} and M_{ez} are the mass penalties for an increased engine offset in the fore/aft and vertical directions, respectively. (A positive fore/aft offset is aft and a positive vertical offset is up.) Thus, the penalty

equation indicates that an offset which reduces the required length of the wing engine pylon results in a decrease in mass. In matrix form, the design equation is

$$\begin{bmatrix} M \\ x \\ y \\ z \end{bmatrix} = \begin{bmatrix} -M_{ey} & -M_{ez} \\ 0.0 & 0.0 \\ 1.0 & 0.0 \\ 0.0 & 1.0 \end{bmatrix} \begin{bmatrix} \Delta y \\ \Delta z \end{bmatrix} + \begin{bmatrix} M_o \\ x_o \\ y_o \\ z_o \end{bmatrix} \qquad (15)$$

Fig. 9 shows the flutter speed and weight versus iteration. The flutter design criteria was not met after 12 iterations. A drop in flutter speed is observed at iteration 6; this is attributed to a poor flutter speed approximation in the design step. The outboard engine proved to have the most impact on flutter with its final offset change, aft and up, at the design limits while the inboard engine moved forward and slightly up. Engine movement closer toward the elastic axis (aft) of the wing indicates an increase in torsion modal frequency. These results indicate that relocating the wing engines in the fore/aft and vertical directions would not, by themselves, completely address the flutter design requirement.

Wing Tip Mass

The wing tip mass was forward of and perpendicular to the elastic axis. The design variable was mass and its initial value was small (0.00001 mugs). A significantly large upper limit was established.

Fig. 9 shows the flutter speed and weight versus iteration history. Convergence was achieved after eight iterations. Thus, we conclude that the addition of a wing tip mass is a viable alternative in addressing the flutter design criteria.

This case has a lower weight penalty than the wing bending stiffness optimization.

Combined Case

All four of the preceding cases were combined in this study of flutter optimization. The design variables are virtually the same as before: wing vertical bending (I_y) stiffnesses, pylon stiffnesses, engine locations and wing tip mass. The only difference in design limits from the other cases is that pylon stiffnesses are not allowed to decrease.

Two flutter optimizations using the combined design variables were performed with the difference between them being the initial wing tip mass.

Run #1 started with the initial design values from the individual studies. Fig. 10 shows the flutter speed and weight versus iteration. The flutter optimization converged after 7 iterations. An increase in flutter speed well above the design speed, with a corresponding weight increase, is observed in iteration 1; this is attributed to a poor flutter speed approximation during the design step.

Interestingly though, the final weight penalty was larger than that of the wing tip mass case. The obvious question is why was not the final design close, if not the same, to the least weight solution given by

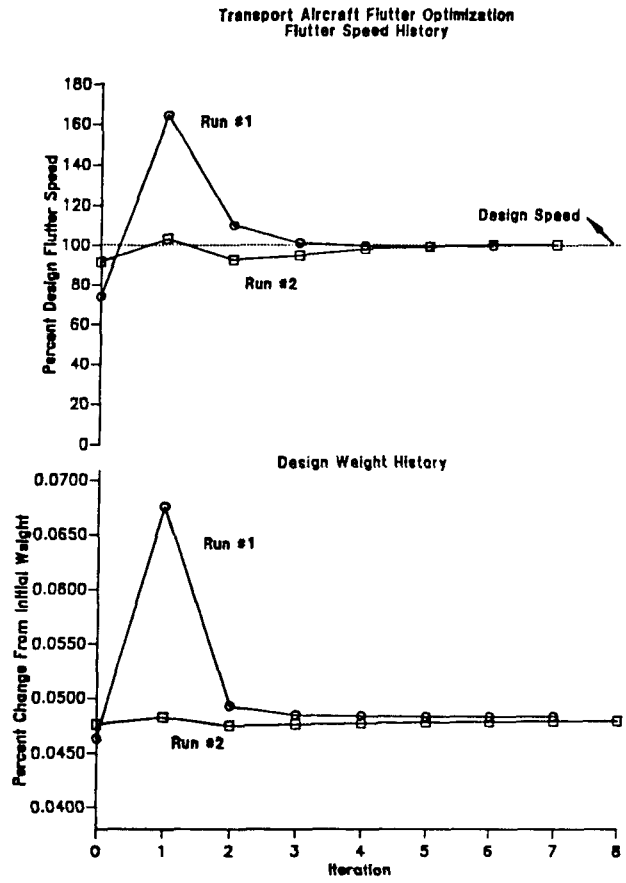

Fig. 10 - Flutter Optimization History -- Combined Cases

the wing tip mass design study? We hypothesized that the design was trapped in a corner formed by the constraint boundaries in design space. Since we knew the "desirable" solution was mass added at the wing tip, we performed another flutter optimization study by giving a substantial, initial wing tip mass in hopes that the design would converge to a more desirable minimum. Figure 10 shows the weight and flutter speed versus iteration. The final design, with 11% less weight penalty than Run #1, was mass primarily added at the wing tip location with a small, aft adjustment of the outboard engine.

Conclusions

This paper demonstrates the flutter optimization technologies implemented in the aeroelastic design optimization program (ADOP) being developed at Douglas Aircraft Company. Additionally, ADOP integrates strength and dynamic modal disciplines into its

design optimization. Buckling and two-bay crack stress allowables, briefly mentioned in this paper, can be included in the design of aircraft structures with their corresponding values and associated weight penalties updated at each iteration.

Three numerical studies in flutter optimization were discussed. They demonstrated ADOP's ability to optimize different design variables including beam bending stiffness, lumped mass value and location, general element stiffness, skin thickness, stringer area, and a combination of these. Multiple flight conditions over three Mach numbers were optimized for flutter. Bilinear design variable linking was also demonstrated.

Extensive technical advances are planned for ADOP. These include optimization of composites, sub-panels, aerodynamic loads, active controls, and stress allowables.

Acknowledgements

The authors wish to express their appreciation to John Galligher, Paul Taylor and Joseph Giesing of Douglas Aircraft for their assistance and valuable expertise.

References

1. Tzong, T.J., Sikes, G.D., Loikkanen, M.J., Giesing, J.P., "Integrated Technologies in Aircraft Design Optimization," *Integrated Technology Methods and Applications in Aerospace Systems Design*, Edited by C.T. Leondes, Academic Press Series of "Control and Dynamic Systems", Vol. 52, to be published.

2. Pickett, R.M., Rubinstein, M.F., and Nelson, R.B., "Automated Structural Synthesis Using a Reduced Number of Design Coordinates," AIAA/ASME/SAE 14th Structures, Structural Dynamics and Materials Conference, Williamsburg, Virginia, March, 1973.

3. Tzong, T.J., Sikes, G.D. and Dodd, A.J., "Large Order Modal Analysis Module in the Aeroelastic Design Optimization Program (ADOP)," MSC 1991 World Users' Conference, Vol. II, Paper No. 36, Universal City, California, March, 1991.

4. Lanczos, C., "An Iteration Method for the Solution of the Eigenvalue Problem of Linear Differential and Integral Operators," *Journal of Research of the Numerical Bureau of Standards*, Vol. 45, October, 1950, pp. 255-282.

5. Parlett, B.N., and Scott, D.S., "The Lanczos Algorithm with Selective Orthogonalization," *Mathematics of Computation*, Vol. 33, 1979, pp. 217-238.

6. Bathe, K.J. and Ramaswamy, S., "An Accelerated Subspace Iteration Method," *Computer Methods in Applied Mechanics ∧ Engineering*, North-Holland Publishing Company, Vol. 23, 1980, pp. 313-331.

7. Tzong, T.J., Sikes, G.D. and Loikkanen, M.J., "Large Order Modal Analysis Techniques in the Aeroelastic Design Optimization Program (ADOP)," SAE Technical Paper Series No. 892323, Aerospace Technology Conference and Exposition, Anaheim, California, September, 1989.

8. Albano, E., and Rodden, W.P., "A Double-Lattice Method for Calculating Lift Distribution on Oscillating Surfaces in Subsonic Flows," *AIAA Journal*, Vol. 7, February, 1969, pp. 279-285.

9. Giesing, J.P., Kalman, T.P., Rodden, W.P., "Subsonic Steady and Oscillatory Aerodynamics for Multiple Interfering Wings and Bodies," *Journal of Aircraft*, Vol. 26, No. 10, October, 1972, pp. 693-702.

10. Bhatia, K.G., "An Automated Method for Determining the Flutter Velocity and the Matched Point," *Journal of Aircraft*, Vol. 11, No. 1., January, 1974, pp. 21-27.

11. Conte, S.D., and de Boor, C., Elementary Numerical Analysis, Second Edition, McGraw-Hill, 1965.

12. MacNeal, R.H., The NASTRAN Theoretical Manual, NASA SP-221(03), March, 1976.

13. Vanderplaats, G.N., Numerical Optimization Techniques for Engineering Design, McGraw-Hill Series in Mechanical Engineering, McGraw-Hill, 1984.

14. DOT USERS MANUAL, Version 2.00, VMA Engineering Inc., Santa Barbara, California, February, 1989.